John von Neumann Institute for Computing

A Bosonic Model for High-Temperature Superconductivity and Antiferromagnetism: Numerical Simulation Studies

A. Dorneich, E. Arrigoni, W. Hanke, M. Troyer,
Shoucheng Zhang

published in

NIC Symposium 2001, Proceedings,
Horst Rollnik, Dietrich Wolf (Editors),
John von Neumann Institute for Computing, Jülich,
NIC Series, Vol. **9**, ISBN 3-00-009055-X, pp. 281-290, 2002.

http://www.fz-juelich.de/nic-series/volume9

A Bosonic Model for High-Temperature Superconductivity and Antiferromagnetism: Numerical Simulation Studies

A. Dorneich[1], E. Arrigoni[1], W. Hanke[1], M. Troyer[2], and Shoucheng Zhang[3]

[1] Institut für Theoretische Physik, Universität Würzburg, Am Hubland, 97074 Würzburg, Germany
E-mail: {ardornei, arrigoni, hanke}@physik.uni-wuerzburg.de

[2] Institut für Theoretische Physik, ETH Zürich, 8093 Zürich, Switzerland

[3] Department of Physics, Stanford University, Stanford, 94305 California

As their most prominent universal feature, high-temperature superconductors always display antiferromagnetism and $d-$wave superconductivity in close proximity, in their phase diagram. A unifying theory has been proposed, according to which these two at first sight radically different phases are "two faces of one and the same coin". They are unified by a common symmetry principle, the SO(5) symmetry. Recently, it was proposed that this theory had to be supplemented with a so-called "Gutzwiller projection" in order to resolve several inconsistencies with experimental results on high-T_c superconductors. Here, we present a numerical study of an effective bosonic model which describes the low-energy physics of this "projected" SO(5) theory. Our numerical results, obtained by the Quantum Monte Carlo technique of Stochastic Series Expansion, show that this model provides a realistic description of the global phase diagram of the high-T_c superconductors and accounts for many of their physical properties. Moreover, we address the question of asymptotic restoring of the SO(5) symmetry at the critical point.

1 Introduction: The SO(5) Theory

The high-temperature superconductors[1,2] (HTSC), discovered at the end of the eighties, are characterized by a number of fascinating properties. The most appealing one, from which their name derives, is the fact that they can conduct electrical current without resistance up to *relatively* high temperatures. In these materials, commonly called cuprates, the dominant charge-carrier dynamics takes place in the two-dimensional (2D) CuO_2-planes[3]. Each CuO_2 unit cell contains an effective magnetic moment of spin $\frac{1}{2}$, essentially due to the Cu ion. At higher temperatures, neighboring Cu-spins form so-called singlets, i. e. pairs of electrons with antiparallel spin (Fig. 1). The energy gain due to the singlet formation, the magnetic exchange J, is relatively large ~ 120meV ~ 1400K. On the other hand, the temperatures (T) for the transition into both low-temperature phases, the antiferromagnetic (AF) and the superconducting (SC) phases, T_N and T_c (see Fig. 1), are both significantly lower and of similar magnitude (~ 250K for T_N and ~ 100K for T_c). Already this order of magnitude suggests that the mechanism of superconductivity does not directly result from the singlet formation, but is instead related to the mechanism, which results in the antiferromagnet in the insulating situation. In addition, the AF and the SC phases are in close proximity in the phase diagram of Fig. 1. Therefore, it seems tempting to look for a common origin for these low-temperature phases, despite the fact that on first glance, they appear dramatically different: On the one hand, the insulator and, on the other hand, the ideal conductor, i.e. the superconductor.

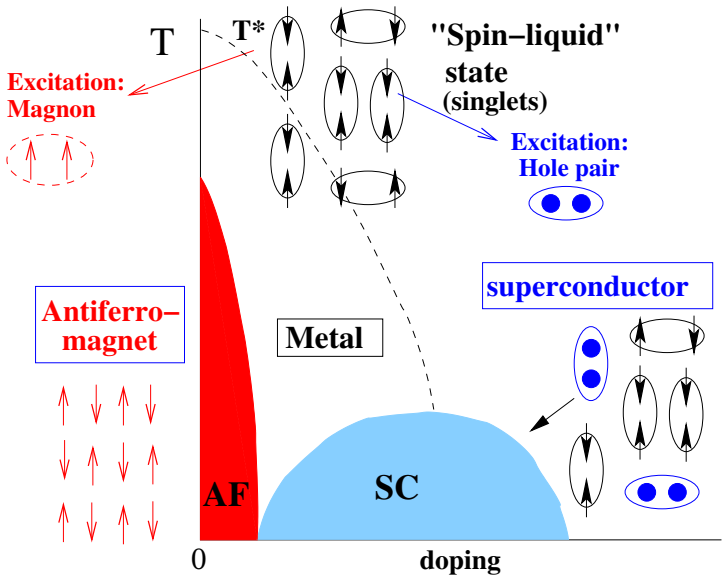

Figure 1. Generic temperature (T) vs. doping phase diagram of the high-temperatures superconductors. The AF (red) and the SC (blue) phases can be seen as a condensation of magnons (red) or hole pairs (blue) on top of the same "spin-liquid" state (see text).

Let us consider, at first, the insulator: At high temperatures $T^* \sim 1000$ K, the singlet pairs are completely disordered. This state is termed, therefore, a spin liquid (Fig. 1). How does one arrive from this disordered state at high temperatures, to an ordered AF state at low temperatures? The idea is that the ordered AF state can be considered as a kind of Bose-Einstein condensation of magnon excitations[4a]. The SC state, on the other hand, corresponds to a Bose-Einstein type of condensation of hole pairs (Cooper pairs). Magnon excitation and hole-pairs excitation are "two faces of one and the same coin" in similarity to other unifying concepts such as the isospin theory of proton and neutron in nuclear physics[5]. The condensation energy of these two excitations yields then the corresponding temperature scales T_N and T_c.

These considerations led S.C. Zhang to formulate the so-called SO(5) theory of HTSC[6]. This theory unifies the three-dimensional order parameter of the AF phase with the two-dimensional SC order parameter. The interpretation of the AF and SC phases of the HTSC within SO(5) theory is as follows: in a completely SO(5)-symmetric system the superspin vector can rotate within a five-dimensional sphere, and we would expect mixed states of coexisting AF and SC long-range order. In reality, however, the chemical potential (which controls the hole doping) induces an anisotropy between AF and d-wave SC and explicitly breaks SO(5) symmetry. The chemical potential in SO(5) theory plays the same role as the magnetic field in angular-momentum with a mechanism symilar to the Zeeman effect.

In summary, the basic idea of SO(5) theory is that antiferromagnetism and superconductivity are "two faces of the same coin" – just as the electric and magnetic field in the

[a] Magnons are electron pairs with parallel spins (Fig. 1)

theory of relativity or the proton and the neutron in Heisenberg's isospin concept[5].

Unfortunately, the presence of a Mott insulating behavior at half-filling (i.e., zero doping) in the cuprates severely challenges the validity of the SO(5) theory[7–10]: SO(5) symmetry requires collective charge pair excitations to have the same (vanishing) mass as collective spin-wave excitations. The real cuprates, on the contrary, are Mott insulators at half-filling and possess a large energy gap U of several eV due to electron-electron interaction. The only way to overcome these problems is to project out states with doubly-occupied sites. These states are separated from the ones without double occupancies by an energy scale of more than 10 eV, which is by orders of magnitude higher than the low-energy scales T_N and T_c. Therefore, states with double occupancies should not even be important as intermediate states for scattering processes. The resulting models are called 'projected SO(5)' or 'pSO(5)' models.

2 "Projected" SO(5) Bosonic Hamiltonian

In Ref.[11] a low-energy effective bosonic model was constructed in which the Gutzwiller constraint of no-double-occupancy was implemented exactly. This is done by projecting out the mode creating particle pair excitations and by retaining only the massless magnon and hole-pair modes. In Ref.[4] it has been shown that the low-energy SO(5) excitations on the rung of a ladder can be cast into a picture of 5 hard-core bond bosons: three magnon states ($t^\dagger_{\alpha=2,3,4}$) and particle and hole-pair state ($t^\dagger_p$ and $t^\dagger_h$, respectively). As an effective coarse-grained model, this description can be extended to a two-dimensional system, whereby the excitations are now defined on a 2×2 plaquette[11]. The Gutzwiller projection is implemented by restricting the Hilbert space to states with $t_p(x) = 0$. The projected SO(5) Hamiltonian takes the form[11]

$$H = \Delta_s \sum_{x,\alpha=2,3,4} t^\dagger_\alpha(x) t_\alpha(x) + (\Delta_c - 2\mu) \sum_x t^\dagger_h(x) t_h(x) \qquad (1)$$
$$- J_s \sum_{<xx'>,\alpha=2,3,4} n_\alpha(x) n_\alpha(x') - J_c \sum_{<xx'>} (t^\dagger_h(x) t_h(x') + \text{h.c.}) \,,$$

where $n_\alpha = (t_\alpha + t^\dagger_\alpha)/\sqrt{2}$ are the three components of the AF order parameter. Δ_s and $\Delta_c \sim U$ are the energies to create a magnon and a hole-pair excitation, respectively, at vanishing chemical potential $\mu = 0$. As one can see, the excitation energy for hole pairs can be compensated by μ in order to have equal energies for spin and hole-pair excitations. Due to this partial compensation, the mean-field ground state of this model[11] recovers SO(5) invariance at $J_c = 2J_s$ and $\Delta_s = \Delta_c$. However, this invariance is not exact, and a symmetry-breaking effect can already be seen at the Gaussian level[11]. Nevertheless, this is the simplest *bosonic* model containing two generic ingredients which are relevant for the high-T_c materials, namely, the Mott gap and the vicinity and, possibly, common origin of the antiferromagnetic and of the superconducting phases.

3 Numerical Analysis

In this Section, we study the physics of the bosonic pSO(5) model introduced in Eq. 1. As already pointed out, numerical simulations are currently the only methods to study

this strongly-correlated system in an appropriate manner, i.e. including all particle-particle interaction effects correctly. Our numerical results for two-dimensional (2D) lattice geometries were obtained by means of Stochastic Series Expansion (SSE, see Ref.[12]). We were able to simulate systems of up to 40×40 lattice sites and to evaluate arbitrary dynamical response functions. Our results show that this model gives a realistic description of the global phase diagram of the high-T_c superconductors and accounts for many of their physical properties. Moreover, we address the question of asymptotic restoring of the SO(5) symmetry at certain critical points of the phase diagram. We carry out our analysis with numerical simulations on an isotropic 2D square lattice, a good model for the physics of the cuprates' CuO_2 planes.

3.1 Doping Dependence of the Chemical Potential and Phase Separation

We choose $J_s = J_c/2$, corresponding to the SO(5)-symmetric point in the mean-field approach[11] and define $J := J_s$ as our unit of energy. We, take $\Delta_s = J$, and shift the chemical potential so that $\Delta_c = \Delta_s$. The mean-field calculation of Ref.[11] predicts a phase transition

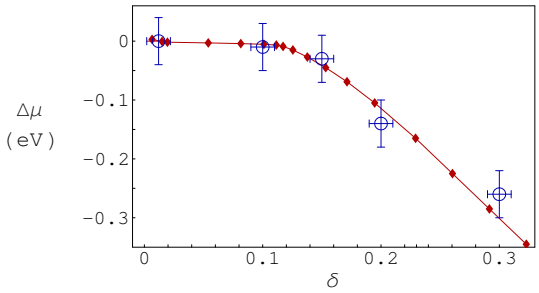

Figure 2. Chemical potential shift $\Delta\mu$ as a function of hole concentration δ (blue circles) for $La_{2-x}Sr_xCuO_4$ at $T = 77$ K. The red diamonds and the solid line show numerical data with $J = 220$ meV and $T \approx 77$ K.

from the AF to the SC phase accompanied by a jump in the hole-pair and magnon densities at a chemical potential $\mu_c = 0$. In mean field, the system at $\mu = \mu_c$ is in a coherently mixed AF+SC phase and there is no phase separation. However, Gaussian fluctuations change the picture and predict a first-order transition. Here, we want to study this region in more detail with an appropriate *strong-coupling* method. In fact, we expect the picture to change appreciably, since no long-range order is allowed in two dimensions. A jump in the density as a function of μ (or, equivalently, a constant μ as a function of density) has also been seen in $La_{2-x}Sr_xCuO_4$[13]. Fig.2 displays a comparison of our numerical calculation with the experimental data of Ref.[13]. As one can see, our data reproduce the experimental results within error accuracy.

The nature of the phase transition at $\mu = \mu_c$ can be determined by studying histograms of the hole-pair distribution for fixed $\mu = \mu_c$. While in an homogeneous phase the density is peaked about its mean value, at $\mu = \mu_c$, we obtain two peaks indicating a first-order transition with a phase separation between (almost) hole-free regions and regions with high hole-pair density. Interestingly, a phase separation into hole-rich and almost hole-

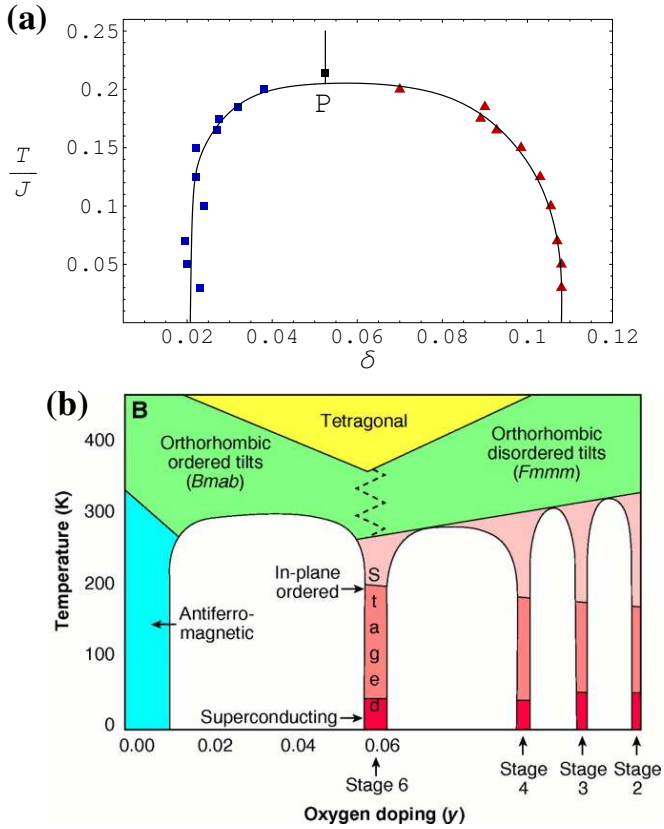

Figure 3. (a) Hole densities of the coexisting phases on the first order transition line from (almost) zero to finite hole density at $\mu = \mu_c$ as a function of temperature. (b) Schematic structure of the "stage 6" phase of La_2CuO_{4+y} at oxygen doping $y \approx 0.06$ (From Ref.[14]).

free phases can also be observed in real cuprates, for example in the HTSC compound La_2CuO_{4+y}[14]. For doping concentrations $y = 0.01$ to 0.055 the material displays a mixture of two phases with different oxygen concentrations: there are alternating AF regions with very low doping concentration ($y = 0.01$) and hole-rich 'stage 6' regions ($y = 0.055$) which become superconducting at low temperatures (Fig. 3b). This is in remarkable accordance with the pSO(5) results in Fig. 3a. Due to the fact that each additional oxygen attracts and immobilizes 2 electrons in the CuO_2 planes, thereby introducing 2 holes, the accordance between theory and experiment is perfect even on a quantitative level: the doping densities of $y = 0.01$ and $y = 0.055$ of the two phases exactly correspond to the values $\delta = 2y = 0.02$ and $\delta = 0.11$ obtained from the pSO(5) model.

3.2 Quasi Long-Range Order and 'Superconducting' Phase

We have anticipated the existence of a SC phase for $\mu > \mu_c$. In fact, in two dimensions at $T > 0$ a true long-range order is prohibited by the Mermin-Wagner theorem. However,

we can still have a so-called Kosterlitz-Thouless[15] (KT) phase of finite superfluid density ρ_s (see below) at finite temperature, which is identified by a power-law decay of the SC correlation function $C_{h(r)}$. The transition separates long-range power-law ($C_{h(r)} \propto r^{-\alpha}$) from rapid exponential decay ($C_{h(r)} \propto \mathrm{e}^{-\lambda r}$). A reliable and accurate distinction between these two decay behaviors requires a finite-size scaling with large system sizes, as well as an efficient Quantum-Monte-Carlo (QMC) estimator for the Green functions appearing in the correlation function. With its non-local update scheme and with our new estimators for arbitrary Green functions, SSE provides both. Fig. 4 demonstrates how precisely a

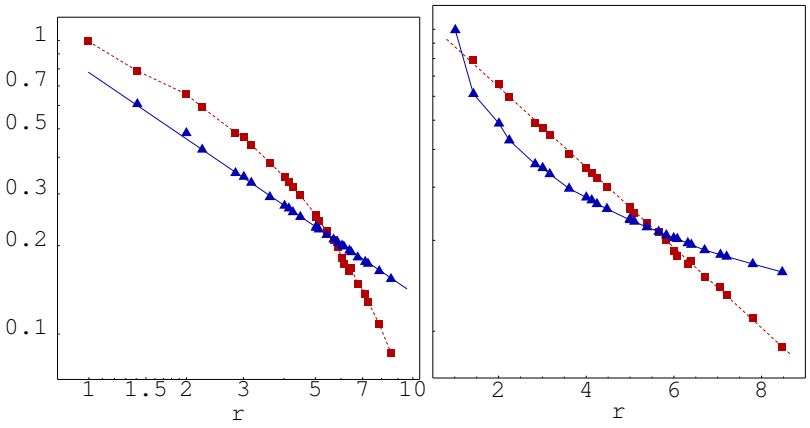

Figure 4. Decay behavior of the SC correlation function $C_{h(r)}$ for $T/J = 0.5$ and for the chemical potentials $\mu = -0.1$ (red squares) and $\mu = 0.3$ (blue triangles). The $C_{h(r)}$ data for $\mu = 0.3$ can be fitted by a straight line in a log-log plot of $\log(C_h)$ versus $\log(r)$ (left), indicating a power-law decay, while an exponential decay can be deduced from the linear fit in a semi-logarithmic plot for the $\mu = -0.1$ data.

correlation length can be determined with SSE. For the point $(T = 0.5J, \mu = -0.1)$, which is located in close neighborhood to the phase transition line in fig. 5 the semi-logarithmic plot almost perfectly fits a straight line, indicating an exponential decay. For the neighbored points $(T = 0.4J, \mu = -0.1)$ or $(T = 0.5J, \mu = 0.1)$ we would find the straight fit in a log-log plot instead of the semi-logarithmic plot, which indicates that these points are located in a different phase with power-law decay behavior of $C_{h(r)}$ (see fig. 5).

In the numerical simulations presented here, the largest system size used for finite-size scaling was 32×32, in some calculations only 24×24 lattice sites. Earlier QMC studies of simpler Hamiltonians than (1), e.g. the analysis of phase transitions in the quantum XY model by Ding[16], needed much larger lattice sites to determine phase transition lines and coherence lengths with high precision. However, the QMC methods employed in those works suffer from systematic Trotter discretization errors and from rapidly growing autocorrelation times on large system sizes, which considerably blows up the statistical errors. In Ding's work[16], for example, typical autocorrelation times on the largest lattice, the 128×128 lattice, were 5000 update–measurement sweeps. Together with the total sweep number of twice $6 \cdot 10^5$, this means that only about 200 statistically uncorrelated data points were recorded, so that the relative statistical error of the QMC results was

about $1/\sqrt{200} \approx 7\%$. In SSE, on the contrary, there are no systematic errors, and the loop update mechanism produces autocorrelation times of the order of 1 even on large lattices. Therefore, the recorded finite-size data typically have relative errors of not more than 10^{-3}. Obviously (see Fig. 4), these high-precision finite-size data allow for a reliable finite-size scaling even on moderate-sized lattices.

Apart from a change in the decay behavior of the superconducting correlation function, there is a second criterion describing the KT transition point: It exploits the fact that the superfluid density jumps from zero to a finite value at the KT temperature T_{KT}[17]. Within QMC methods, the superfluid density can be measured quite easily by counting *winding numbers*[18–20]. In two dimensions the superconducting density ρ_s is given in terms of the mean-squared winding number $\langle \mathbf{W} \rangle$ via $\rho_s = \frac{m\, k_B\, T}{\hbar^2} \frac{\langle \mathbf{W}^2 \rangle}{2}$ In finite-cluster simulations, the jump of ρ_s from zero to a finite value at the KT transition point can be detected more easily than the change in the decay behavior of the correlation function itself. Fig. 5 plots

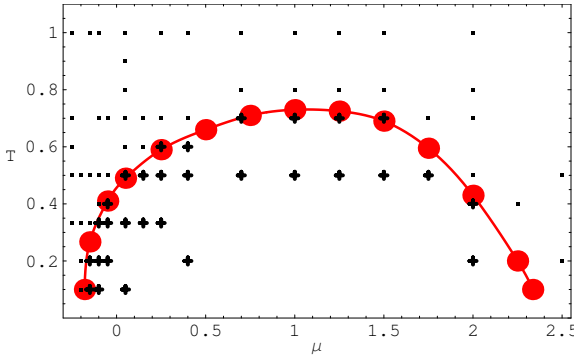

Figure 5. Location of the superconducting phase transition in the projected SO(5) model: The black points identify the long-distance decay behavior of the SC correlation function, the small dots corresponding to an exponential decay, while the crosses indicate a power-law decay. The connected red circles trace the transition temperature from the jump in the boson phase stiffness in the infinite-volume limit. This behavior should be compared with the typical dependence of the critical superconducting temperature versus doping (red region of Fig. 1)

the phase diagram obtained by applying both criteria independently. The figure shows that the projected SO(5) model indeed has a KT phase with quasi long-range order whose form in μ-T space looks like the one of the high-T_c cuprates. Both criteria result in exactly the same clearly pronounced phase-separation line.

3.3 Spin Resonance Peak

One of the main features of SO(5) theory is that it provides an elegant explanation for the neutron resonance peak observed in some high-T_c cuprates at $k = (\pi, \pi)$[6]. Experiments show that the resonance energy ω_{res} is an increasing function of T_c, i.e. ω_{res} increases as a function of doping in the underdoped and decreases in the overdoped region[21]. Here, we address the question whether the T_c dependence of ω_{res} can be reproduced within the projected SO(5) model. To this purpose, we study the spin correlation function at $k = (\pi, \pi)$.

Fig. 6 shows the spin correlation spectrum obtained from the projected SO(5) model in two dimensions as a function of the chemical potential.

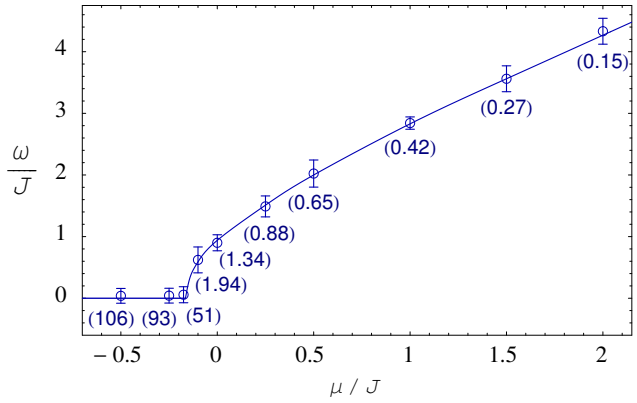

Figure 6. Dispersion of the (π, π)-peak of spin correlation as a function of the chemical potential The numbers in parentheses indicate the peak weights, i.e. the area under the peak.

The magnon-dominated paramagnetic region and the underdoped SC region are described correctly: spin-wave excitations are essentially massless Goldstone modes in the magnon-dominated phase at $\mu < \mu_c$ and become massive when entering into the SC phase. The resonance energy $\omega_{\rm res}$ increases monotonically up to optimal doping $\mu_{\rm opt} \approx 1$. On the other hand, the SO(5) theory is not expected to describe the system too far away from the AF/SC transition, i. e. in the overdoped regime. Notice that the resonance peak continuously looses weight when increasing μ, which is consistent with experimental observations[21].

A comparison of the critical temperature T_c obtained from Fig. 5 and $\omega_{\rm res}$ at optimal doping yields the ratio $T_c/\omega_{\rm res,opt} = 0.23$. This is again in accordance with the corresponding ratio for $YBa_2Cu_3O_{6+x}$, for which the experimentally determined values $T_c = 93\,{\rm K}$ (thus $k_B T_C = 8.02$ meV) and $\omega_{\rm res,opt} = 41$ meV yield $T_c/\omega_{\rm res,opt} = 0.20$.

3.4 How SO(5)-Symmetric is the pSO(5) Model?

So far we have presented some general properties of the pSO(5) model in two dimensions. The question "how SO(5)-symmetric is the pSO(5) model", i.e. the question whether there exists a point for which the full SO(5)-symmetry is dynamically restored, still remains open. As one can see from Eq. (1), the excitation energy for hole pairs can be compensated by μ, in order to have equal energies for *local* spin and hole-pair excitations. Due to this partial compensation the mean-field ground state of this model recovers exact SO(5) invariance at $J_c = 2\ J_s$ and $\Delta_s = \Delta_c$[11]. However, this invariance is not exact, and a symmetry-breaking effect can already be seen at the Gaussian level[11]. For a *classical* three-dimensional SO(5)-symmetric model, numerical simulations indicate that the symmetry is asymptotically restored at a bicritical point provided the symmetry-breaking terms have the appropriate sign[22,23]. This is in contrast with the prediction from the ϵ-expansion[24],

which would suggest a fluctuation-induced first-order transition. The discrepancy clearly indicates that *strong-coupling* effects play an important role, calling for an appropriate, i.e. numerically exact treatment, as it is provided by SSE. This assumption is further supported by a recent work by A. Aharony[25].

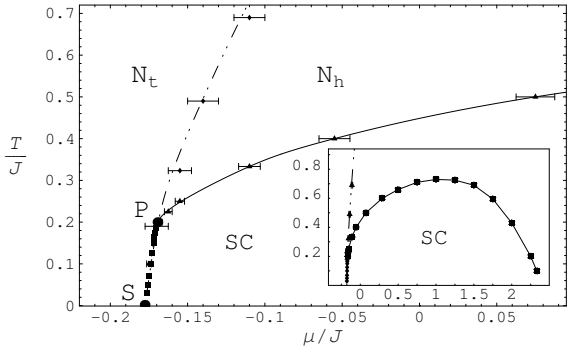

Figure 7. Phase diagram of the pSO(5) model: The squares between S and the tricritical point P trace the first-order line of phase separation. The solid line from P to the right edge of the plot traces the Kosterlitz-Thouless transition between the "SC" and the normal state. The dashed line separating N_t (=magnon dominated region) and N_h (=hole pair dominated region) describes the line of equal AF and SC correlation lengths. The small inlay shows the same phase diagram on a larger μ scale, covering the whole "SC" KT phase.

One necessary condition for an SO(5)-symmetric point is that the formation energies of hole-pair bosons and of magnons are identical. This condition is fulfilled along the line from S to the tricritical point P in Fig. 7. Another necessary condition is that hole pairs and magnons behave in the same way at long distances. This condition is fulfilled on the dashed line in Fig. 7, where the AF and SC correlation lengths ξ become equal. Interestingly, these two conditions meet (within error bar accuracy) at the tricritical point P. Although here the correlation length is still finite, we find relatively large ξ values of order 10 to 15 in the immediate vicinity of point P, demonstrating the importance of SO(5) critical fluctuations in this region.

The asymptotic restoring of SO(5) symmetry in the vicinity of the critical point cannot be conclusively answered in $D=2$ dimensions, even though we have found a critical-point scenario which makes asymptotic restoring of SO(5) symmetry at a $T \neq 0$ bicritical point in $D=3$ a good possibility. For that reason (and because there exists no AF phase at finite temperature in $D=2$) it would be interesting to analyze the model in three dimensions.

4 Summary

In summary, we have shown that the projected SO(5) model in two dimensions – or more general four-boson models of type Eq.(1), can be considered as a generic model for the high-temperature superconducting materials. It gives a semiquantitative or even quantitative description of many properties of the HTSC in a consistent way. In particular, we have identified an AF and a SC phase whose bounds look similar to the the ones of the real cuprate materials. Also, the doping dependence of the chemical potential as well as that of

the neutron-resonance peak in the underdoped regime are reproduced correctly. Furthermore, the pSO(5) model reproduces physical effects like phase separation or coexistence of antiferromagnetism and superconductivity.

Acknowledgments

The authors acknowledge financial support from BMBF (05SB8WWA1), DFG [(HA 1537/17-1) as well as from the Heisenberg program (AR 324/3-1)], KONWIHR OOPCV and the Swiss National Science Foundation. The calculations were carried out on a Cray T3E at the high-performance computing center HLRZ (Jülich) and required a total amount of about 1.5×10^5 CPU hours.

References

1. J. G. Bednorz and K. A. Müller, Zeit. Phys. B **64**, 189 (1986).
2. P. W. Chu, Scientific American **September**, 128 (1995).
3. D. S. Marshall, D. S. Dessau, A. G. Loeser, C.-H. Park, A. Y. Matsuura, J. N. Eckstein, I. Bozovic, P. Fournier, A. Kapitulnik, W. E. Spicer, and Z.-X. Shen, Phys. Rev. Lett. **76**, 4841 (1996).
4. R. Eder, A. Dorneich, M. G. Zacher, W. Hanke, and S.-C. Zhang, Phys. Rev. B **59**, 561 (1999).
5. W. Heisenberg, Z. Phys. **77**, (1932).
6. S.-C. Zhang, Science **275**, 1089 (1997).
7. M. Greiter, Phys. Rev. Lett. **79**, 4898 (1997).
8. S. Meixner, W. Hanke, E. Demler, and S.-C. Zhang, Phys. Rev. Lett. **79**, 4902 (1997).
9. G. Baskaran and P. W. Anderson, J. Phys. and Chem. Solids **59**, 1780 (1998).
10. S.C. Zhang, J. Phys. and Chem. of Solids **59**, 1774 (1998).
11. S.-C. Zhang, J.-P. Hu, E. Arrigoni, W. Hanke, and A. Auerbach, Phys. Rev. B **60**, 13070 (1999).
12. A. Dorneich and M. Troyer, Phys. Rev. E **64**, 066701 (2001).
13. A. Ino, T. Mizokawa, A. Fujimori, K. Tamasaku, H. Eisaki, S. Uchida, T. Kimura, T. Sasagawa, and K. Kishio, Phys. Rev. Lett. **79**, 2101 (1998).
14. B. O. Wells, Y. S. Lee, M. A. Kastner, R. J. Christianson, R. J. Birgeneau, K. Yamada, Y. Endoh, and G. Shirane, Science **277**, 1067 (1997).
15. J. M. Kosterlitz, J. Phys. C **7**, 1047 (1974).
16. H.-Q. Ding, Phys. Rev. B **45**, 230 (1992).
17. D. R. Nelson and J. M. Kosterlitz, Phys. Rev. Lett. **39**, 1201 (1977).
18. E.L. Pollock and D.M. Ceperley, Phys. Rev. B **36**, 8343 (1987).
19. K. Harada and N. Kawashima, Phys. Rev. B **55**, R11949 (1997).
20. M. Troyer and S. Sachdev, Phys. Rev. Lett. **81**, 5418 (1998).
21. H.F. Fong, P. Bourges, Y. Sidis, L.P. Regnault, J. Bossy, A. Ivanov, D.L. Milius, I.A. Aksay, and B. Keimer, Phys. Rev. B **61**, 14773 (2000).
22. E. Arrigoni and W. Hanke, Phys. Rev. B **62**, 11770 (2000).
23. X. Hu, Phys. Rev. Lett. **87**, 057004 (2001).
24. J. M. Kosterlitz, D. R. Nelson, and M. E. Fisher, Phys. Rev. B **13**, 412 (1976).
25. A. Aharony, Phys. Rev. Lett. **88**, 059703 (2002).